

Accepted Manuscript

Dibucaine in ionic-gradient liposomes: biophysical, toxicological and activity characterisation

Veronica M. Couto, Maria J. Prieto, Daniela E. Igartúa, Daniela A. Feas, Lígia N.M. Ribeiro, Camila M.G. Silva, Simone R. Castro, Viviane A. Guilherme, Darlene D. Dantzger, Daisy Machado, Silvia del V. Alonso, Eneida de Paula

PII: S0022-3549(18)30314-9

DOI: [10.1016/j.xphs.2018.05.010](https://doi.org/10.1016/j.xphs.2018.05.010)

Reference: XPHS 1164

To appear in: *Journal of Pharmaceutical Sciences*

Received Date: 5 January 2018

Revised Date: 6 April 2018

Accepted Date: 17 May 2018

Please cite this article as: Couto VM, Prieto MJ, Igartúa DE, Feas DA, Ribeiro LNM, Silva CMG, Castro SR, Guilherme VA, Dantzger DD, Machado D, Alonso SdV, de Paula E, Dibucaine in ionic-gradient liposomes: biophysical, toxicological and activity characterisation, *Journal of Pharmaceutical Sciences* (2018), doi: 10.1016/j.xphs.2018.05.010.

This is a PDF file of an unedited manuscript that has been accepted for publication. As a service to our customers we are providing this early version of the manuscript. The manuscript will undergo copyediting, typesetting, and review of the resulting proof before it is published in its final form. Please note that during the production process errors may be discovered which could affect the content, and all legal disclaimers that apply to the journal pertain.



**Dibucaine in ionic-gradient liposomes: biophysical, toxicological and activity
characterisation**

Veronica M. Couto^a; Maria J. Prieto^b; Daniela E. Igartúa^b; Daniela A. Feas^b; Lígia N. M. Ribeiro^a;
Camila M. G. Silva^a; Simone R. Castro^a; Viviane A. Guilhermé^a; Darlene D. Dantzger^a; Daisy
Machado^a; Silvia del V. Alonso^b; Eneida de Paula^{a,*}

^a Department of Biochemistry and Tissue Biology, Institute of Biology, University of Campinas, Campinas, SP, Brazil.

^b Laboratory of Biomembranes, Department of Science and Technology, Structure Biology and Biotechnology group, National University of Quilmes, IMBICE-CONICET, Bernal, BA, Argentina.

* Corresponding author: Eneida de Paula, Department of Biochemistry and Tissue Biology, Institute of Biology, University of Campinas (Unicamp), 13083-862, Campinas, SP, Brazil; e-mail: depaula@unicamp.br

ABSTRACT

Administration of local anaesthetics (LA) is one of the most effective pain control techniques for postoperative analgesia. However, anaesthetic agents easily diffuse into the injection site, limiting the time of anaesthesia. One approach to prolong analgesia is to entrap LA in nanostructured carriers (e.g. liposomes). Here we report that using an ammonium sulphate gradient was the best strategy to improve the encapsulation (62.6%) of dibucaine (DBC) into liposomes. Light scattering and nanotracking analyses were used to characterise vesicle properties, such as, size, polydispersity, zeta potentials and number. *In vitro* kinetic experiments revealed the sustained release of DBC (50% in 7 h) from the liposomes. Additionally, *in vitro* (3T3 cells in culture) and *in vivo* (zebrafish) toxicity assays revealed that ionic-gradient liposomes were able to reduce DBC cyto/cardiotoxicity, as well as morphological changes in zebrafish larvae. Moreover, the anaesthesia time attained after infiltrative administration in mice was longer with encapsulated DBC (27 h) than with free DBC (11 h), at 320 μM (0.012%), confirming it as a promising long-acting liposome formulation for parenteral drug administration of dibucaine.

Keywords: liposomes, encapsulation, toxicity, controlled release/delivery, injectables, stability, formulation.

Abbreviations: ammonium sulphate gradient liposomes (LUV AS); ammonium sulphate gradient liposomes with dibucaine (LUV_{DBC}AS); area under the effect curve (AUEC); conventional liposomes (LUV 7.4); conventional gradient liposomes with dibucaine (LUV_{DBC}7.4); dibucaine (DBC); drug delivery system (DDS); days post fertilisation (dpf); dynamic light scattering (DLS); encapsulation efficiency (%EE); hour post treatment (hpt); large unilamellar vesicles (LUV); local anaesthetic (LA); maximum possible effect (%MPE); methyl thiazolyl tetrazolium (MTT); nanoparticle tracking analysis (NTA); pH gradient liposomes (LUV 5.5); pH gradient liposomes with dibucaine (LUV_{DBC}5.5); polydispersity index (PDI); zeta potential (ZP).

INTRODUCTION

Pain management is still an on-going issue, especially in intensive care units.¹ Moderate to severe postoperative pain was experienced by many patients who underwent orthopaedic, maxillofacial, breast, inguinal hernia, or varicose vein surgeries, amongst others.² The use of local anaesthetic (LA) wound infiltration for postoperative analgesia has been demonstrated to be a highly effective pain control technique.³⁻⁵ Additionally, LA relieves pain without eliciting undesirable side effects, unlike systemic analgesics⁶. The main limitation to their widespread usage is the short effect duration (2–6 hours), which requires repeated administration, leading to a reduction in patient compliance.²

One approach to prolong analgesia is to entrap the LA into a drug delivery system (DDS), that can act as a reservoir at the site of injection.^{7,8} Since 1970, liposomes have been tested as carriers for hydrophilic and lipophilic drugs.⁹ Liposomes are composed of phospholipids, which self-enclose to form vesicles encompassing one or more aqueous cores.^{10,11} Currently, there are 13 liposome-based drugs approved by US FDA and a great number are in various stages of clinical trials.¹²

Dibucaine (DBC) is an amino-amide LA of high potency. It is mainly used as a topical active agent, in haemorrhoid creams and ointments. In order to achieve higher DBC encapsulation in liposomes, we have used the remote-loading technique. In this approach, a weak base such as DBC, is actively entrapped into the liquid core of preformed ionic-gradient liposomes.¹³ Some examples of the successful application of the remote-loading technique are the commercial liposomal products Doxil, Myocet, and DaunoXome. Notably, Doxil was the first liposomal drug approved by the FDA for infiltrative cancer treatment in 1995.¹⁴

In the remote-loading technique, liposomes exhibit a transmembrane pH gradient: the internal vesicle solution is acidic, while the external solution is kept at pH 7.4. The drug is added to the external liposomal medium. Neutral molecules are able to diffuse from this medium into the liposomes, where they become protonated and subsequently trapped as only the uncharged form is membrane permeable.¹⁵ An ionic gradient can be created using a low-pH buffer (pH 5.5) or ammonium sulphate in the inner aqueous core of the liposomes. In the latter, the ammonium ions in solution deprotonate to form ammonia (which crosses the membrane), while the protons that remain drive the weak-base uptake.^{16,17} Remote loading is one of the best approaches for achieving a high drug encapsulation into liposomes.¹³ It has also shown to be efficient for the sustained delivery of LA, including bupivacaine⁶ and ropivacaine.^{17,18} The sustained release of the anaesthetics limits their clearance, decreasing the risk of systemic toxicity,^{19,20} and prolonging their potency. The liposomal formulation of

bupivacaine (Exparel) in the market, is both the only and an expensive option for long-acting postoperative local anaesthetic treatment.²¹ The safety profile and efficacy of this product is still being established.²² Dibucaine is a potent local anaesthetic and it is more effective than bupivacaine or ropivacaine (for which IGL has been described). Therefore, a new formulation of long-acting DBC is an interesting proposal for post-surgical pain management.

In the present work, we describe the development and characterisation of a remote-loaded dibucaine liposome formulation, proposed as a potential long-acting DDS for the treatment of postsurgical pain. *In vitro* and *in vivo* toxicity tests suggest that it is non-toxic and safe to use. Antinociceptive tests revealed a remarkable increase in anaesthesia time (longer than a day), accomplished with this unique infiltrative formulation for dibucaine.

MATERIALS AND METHODS

Hydrogenated soy phosphatidylcholine (HSPC) was purchased from Avanti Lipids Inc. (Alabaster, AL, USA). Cholesterol, HEPES, sodium acetate, and uranyl acetate were purchased from Sigma Chem. Co. (St. Louis, MO, USA). Dialysis tubing membrane 12000-1400KDA MWCO was purchased from Spectrum (Los Angeles, CA, USA). Ammonium sulphate was acquired from Merck (São Paulo, SP, Brazil) and dibucaine hydrochloride was kindly donated by Althaia Ltda (Atibaia, SP, Brazil).

Preparation of liposome formulations

Liposomes composed of HSPC and cholesterol (2:1 mol%) were produced at a final lipid concentration of 5 mM. The lipids in chloroform solution were dried to form a thin lipid film. Then, the film was hydrated with either 50 mM HEPES buffer (pH 7.4), 50 mM acetate buffer (pH 5.5) or 300 mM $(\text{NH}_4)_2\text{SO}_4$. The formulations were stirred for 10 min and extruded through polycarbonate membranes (400 nm) to produce large unilamellar vesicles (LUV). The external medium was replaced by 50 mM HEPES buffer (pH 7.4), after phase separation (centrifugation at $130,000 \times g$, for 2 h, at 4 °C). Then, DBC (320 μM) was actively loaded into the vesicles, at room temperature.^{16,17}

Liposome characterisation

The stability of the formulations was investigated by measuring the vesicle size and concentration, polydispersity index (PDI), and zeta potential (ZP) during 6 months of storage at 4 °C. Size, PDI and ZP were determined in a Zetasizer Nano ZS90 (Malvern, Worcestershire, UK) dynamic light scattering (DLS) analyser. The samples were diluted in deionised water and measured three times at 25 °C.

Measurements of particle size and concentration were also carried out in nanoparticle tracking analysis (NTA) equipment (NanoSight NS300, Malvern, Worcestershire, UK) equipped with a sample chamber and a 532 nm (green) laser. The samples were diluted in deionised water and measured three times, for 60 s. The temperature was kept constant at 25 °C during the experiment.

Encapsulation efficiency

The encapsulation efficiency (EE%) of dibucaine was determined by the ultrafiltration/centrifugation method, using a 10 kDa regenerated cellulose ultrafiltration device (Millipore Corp., Billerica, MA, USA). The liposome samples in the device were centrifuged at 12 °C, for 20 min at 4,100 × g. DBC quantification in the filtrate was determined by HPLC, in a ProStar 410 (Varian, Palo Alto, CA, USA) at 241 nm and 35 °C, using a C18-reversed-phase column (125 mm × 4 mm), 30 µL injection volume, acetonitrile:triethylamine phosphate buffer (55:45 v/v) mobile phase and 1.0 mL/min flow rate.²³ The encapsulation efficiency was calculated according to equation 1:

$$\%EE = (1 - \text{Drug}_{\text{untrapped}} / \text{Drug}_{\text{total}}) \times 100 \quad (1)$$

In vitro dibucaine release from the liposomes

The *in vitro* release of DBC (free or encapsulated in liposomes) was performed on Franz diffusion cells using a dialysis membrane (SpectraPor 12000–14000 Da MWCO). 400 µL of DBC (320 µM, in solution or encapsulated in the liposome formulations) was applied to the donor compartment, which was separated from the receptor compartment by a dialysis membrane. The receptor medium, containing 4 mL of HEPES buffer (pH 7.4) was kept at 37 °C and stirred at 300 rpm. Each test was run for 24 h and samples (300 µL) from each cell (n = 6) were withdrawn at 0.25, 0.5, 1, 2, 3, 4, 5, 7, 9 and 24 h. Each withdrawn sample was immediately replaced with the same volume (300 µL) of buffer that was reintroduced into the receptor chamber. The KinetDS v3 software was applied to process the whole dataset using different theoretical release models. The determination coefficient

(r^2) was used to define the best-fit model, expressed as squared Pearson's correlation coefficient. In particular, the Weibull model followed equation 2:

$$m = 1 - \exp \left[\frac{-(t)^b}{a} \right] \quad (2)$$

Where: m is the amount of drug released, a is the time constant, and b the shape parameter.²⁴

Cell viability test

The *in vitro* cytotoxicity of DBC (in solution or encapsulated into the liposomes) was measured using the methyl thiazolyl tetrazolium (MTT) assay, in cultures of BALB/c 3T3 cells. The fibroblasts, at a density of 1×10^4 cells/mL, were seeded in 96-well culture plates and incubated for 24 h at 37 °C and 5% CO₂. The RPMI culture medium was then removed and replaced with 100 µL of fresh medium containing different concentrations of the samples (liposomes, dibucaine or liposomal dibucaine). Untreated cells were used as controls. After the exposure period (2 h), the medium was removed and the plate was washed with phosphate-buffered saline (pH 7.4). The medium (100 µL, without serum) with 0.5 mg/mL of MTT reagent was added to each well and incubated for 3 h at 37 °C. The MTT solution was discarded from each well and 100 µL of ethanol was added to dissolve the formazan crystals. The formazan absorbance was measured at 570 nm. Results were expressed as the mean viability percentage ± standard error means (SEM). Experiments were performed in triplicate.

Bioassays

Male Swiss mice (30–35 g) were obtained from CEMIB-UNICAMP (Centro de Bioterismo, University of Campinas, UNICAMP, Brazil) and housed in standard cages under a 12/12 h light/dark cycle. All experiments were approved by Institutional Animal Care and Use Committee (protocol # 2991-1).

Wild-type adult zebrafish (8–12 months old) were kept in a glass aquarium filled with filtered tap water at 28 ± 1 °C under a 14/10 h light/dark cycle, in accordance with the OECD (Fish Embryo Acute Toxicity, FET Test 236, 2013). At one day post fertilisation (1 dpf), the fertilised eggs were transferred into 96-well plates (1 embryo per well) and conditioned in E3 medium (NaCl 0.29 g/L, KCl 0.012 g/L, CaCl₂ 0.036 g/L and MgSO₄ 0.039 g/L in

deionised water, and 50 ppb methylene blue to inhibit fungal growth). The Institutional Animal Care Committee of the Universidad Nacional de Quilmes (Buenos Aires, Argentina) approved the protocol (CE-UNQ 2/2014).

In vivo toxicity tests in zebrafish

The toxicity of the ionic-gradient liposomal DBC formulation was evaluated using zebrafish (*Danio rerio*) larvae, as an *in vivo* model. At 5 days after fertilisation (dpf), larvae were treated with sublethal doses of free DBC and liposome formulation (with or without DBC) for the following tests (Figure 1). Untreated larvae were used as controls.

Anaesthesia evaluation in zebrafish larvae

The anaesthetic effect caused by an acute dibucaine dose was evaluated in 5 dpf zebrafish larvae. The experimental animals (n = 24) were exposed to 32 μ M DBC (free or encapsulated in the ionic-gradient liposomes) for 2 h. Then, the medium was replaced with fresh E3 medium and the post-anaesthetic recovery period was monitored with a Leica Zoom 2000 (Wetzlar, Germany) microscope, for the first 10 h, and after 24 h e 48 h. The anaesthetic effect was tested by applying a slight pressure to the body of the larvae with the help of a needle (BD 21G, 0.8 mm). The larvae were considered anesthetised when they did not react to the pressure or attempt to swim away.

Cardiotoxicity test

After 48 h of treatment, the heart rate of zebrafish was determined (at 7 dpf larvae). Control and experimental larvae were individually recorded for 15 seconds, with a trinocular microscope (SMZ800, Nikon, Tokyo, Japan). Heartbeats were manually counted to determine the mean heart rate, which was then expressed as a percentage relative to the heart rate of the control (non-treated larvae). Experiments were performed on eight larvae per group (n = 8).²⁵

Zebrafish motor behaviour

To evaluate the effect of increasing DBC concentration on zebrafish locomotor activity, the larvae were recorded for 15 min at 4 h, 24 h, and 48 h post treatment (hpt) with dibucaine (free or in the liposome formulation).

The recording system used was an infrared device that detects light refraction through the zebrafish body. A transient fluctuation in the signal was generated when larvae moved across the light beam. The outputs of the light signals were digitised by a multi channel ADC system (WMicrotracker; Design plus SRL, Buenos Aires, Argentina) and processed by dedicated software programmed in MS-Visual Basic. Motor activity was calculated as the sum of the activity events during 15 min, relative to the control. Experiments were performed three times, on eight larvae per group (n = 24).

Morphological changes in different organs

Images of 7 dpf larvae were captured using a trinocular microscope (Nikon SMZ800/Microsoft Camera). The assay employed to record morphological anomalies, used the numerical score system proposed by Panzica-Kelly and colleagues,²⁶ with modifications: 5 (structure is entirely normal), 4 (structure is within the normal range), 3 (mild anomaly), 2 (moderate anomaly), and 1 (severe anomaly). Feature analysis included tail, heart, face, brain, and jaw. Morphological changes were calculated as the sum of the score for each feature, normalised to the control (n = 8).

Anaesthesia evaluation in mice: tail flick test

The tail-flick test was conducted to evaluate the duration of analgesia in mice exposed to a focused thermal stimulus (55 ± 1 °C, 150 W).²⁷ First, the mice were gently placed in an acrylic restraint chamber with an opening, to allow the tail to protrude. After which, the tail was exposed to heat from a light beam, and the time (in seconds) until the tail flicks (latency time) was recorded. A 15-second cut-off period was adopted, to avoid thermal injury. On the day before the injection, baseline testing was performed. Then, 40 μ L of the sample containing 320 μ M DBC (free or in liposome formulation) was injected into the root of the mouse-tail. The test was performed 15, 30, and 45 min after injection, as well as every 2 h, for as long as the sensory block (latency > baseline) was registered. The same observer performed all the experiments. Data were expressed as the percentage of maximum possible effect (%MPE), duration of the analgesic effect (min), and area under the effect curve (AUEC) for each experimental group. % MPE was calculated according to equation 3. AUEC values were calculated by the integral, in a plot of drug effect vs. time, starting from the first time value in the data set and ending at the last time value.

$$\%MPE = \frac{(\text{test latency time} - \text{baseline})}{(\text{cut-off} - \text{baseline})} \times 100$$

(3)

Statistical analysis

The data were analysed using GraphPad Prism v6.01 (Northampton, MA, USA). The Student's t-test was used to evaluate statistical significant differences in the particle size, PDI, and zeta potential data of the liposome formulations (with vs. without DBC; or at initial vs. time) during the stability studies. One-way ANOVA with the post-hoc Tukey multiple comparison test was used to analyse the data from the encapsulation efficiency, cell viability and tail-flick tests. The *in vivo* toxicity tests were analysed by one-way ANOVA, followed by Dunnett's post-test. Statistical significance was defined as $p < 0.05$.

Results and discussion

Liposome characterisation

Appropriate size characterisation of a nanostructured DDS is an important safety assessment in the development of a novel parenteral formulation.²⁸ Two powerful techniques, DLS and NTA, were performed to obtain such information (Table 1, Figure 2). The initial physicochemical characterisation by DLS revealed liposomes sizes were in the region of 380 nm (Table 1). Also in table 1, NTA results are shown as the size distribution width (D90, D50, and D10) calculated by the cumulative size distribution, plus nanoparticles concentration.

Comparing the DLS and NTA size distributions it becomes evident that the results are quite similar for the formulations with monodisperse size distribution, such as that of LUV 7.4 ($PDI \leq 0.2$, see Figure 2A). However, in the case of polydisperse size distributions, as observed for the pH-gradient formulation and sulphate-gradient formulation (Figure 2B–C), the results obtained from both techniques were significantly different. This is because DLS measurements consider the intensity of the light scattered by all particles, at the same time. Therefore, the presence of a small number of large particles, which scatter light more intensely than the small particles, might lead to the average size being biased towards the larger particles.²⁹ On the other hand, NTA follows particle-by-particle (individual) movements, avoiding the bias described for DLS; this also explains why NTA mean diameters

were always smaller than those measured by DLS. In addition, the incorporation of DBC significantly increased the size of the ionic-gradient liposomes (LUV 5.5 and LUV AS), but not that of the conventional liposomes (LUV 7.4), as confirmed by both (DLS and NTA) techniques.

DLS measurements were also used to follow the stability of the formulations, as shown in Figure 2. During six months of storage, all the formulations presented some statistical differences in size and PDI over time but, there were no instances where the mean size exceeded 455.6 nm (Fig. 2 A-C), and thus are suitable for infiltrative anaesthesia use.³⁰

Figure 2D also shows that DBC upload significantly decreased the absolute (negative) zeta potential values of the conventional liposomes (LUV_{DBC}7.4) during the 180 days of storage. Changes in zeta potential indicate that DBC partitions into the liposome bilayer, staying at the surface of the liposomes as also reported by Kuroda and colleagues,³¹ hence being able to affect the surface electric potential of the nanoparticles. They used ¹H-NMR to demonstrate that DBC was superficially inserted in-between the lipids, at the polar head group region of egg phosphatidylcholine liposomes. Such an effect was not so evident for the gradient liposomes (LUV_{DBC}5.5 and LUV_{DBC}AS), in which absolute zeta values were smaller (closer to zero), indicating inferior physical stability for those nanoparticles. Despite of that, no significant pH changes (7.41 ± 0.05) were observed during the storage of any of the tested formulations (data not shown).

The differences in Zeta values also help to explain the different fluctuations in size and PDI of the liposomes. After 180 days of storage, the average zeta potential of LUV_{DBC}5.5 (in module) was significantly smaller (-5 mV) than that of LUV_{DBC}AS (-10 mV) or LUV_{DBC}7.4 (-20 mV), as shown in Fig. 2D. Therefore, in the first (pH gradient formulation), the repulsive forces between the vesicles are weaker and some aggregation may have happened, increasing the average size of the particles. This is more evident during the storage, when LUV_{DBC}5.5 has shown the larger fluctuations in size, PDI and Zeta (Fig. 2).

The stability tests were also performed using NTA, which contributed with another parameter, not so commonly used, but of maximum importance in the characterisation of DDS,³² namely particle concentration, as shown in Table 1 and Figure S1 (Supplementary Material). The number of particles, in the range of $1-6 \times 10^{12}$ liposomes/mL, did not vary significantly during storage, in agreement with the discrete particle size changes observed (Fig. S1). For instance, if the liposomes were unstable and underwent fusion over time, the number of particles would decrease, while the average size would increase. Moreover, the measured number of tracked particles is also compatible with the number of liposomes (3×10^{12} liposomes/mL) expected for a 5 mM

suspension of 190 nm vesicles (as calculated from the LUV bilayers' surface area, divided by the area/lipid – 5.5 Å²).^{18,33}

Encapsulation efficiency

The remote-loading technique was used as a strategy to entrap suitable amounts of DBC inside of the liposomes. We created two types of ionic gradients (pH and ammonia-driven) that made the inner liposome aqueous core acidic, while the external pH was kept at pH 7.4. Table 1 shows that among the formulations tested, the highest DBC encapsulation efficiency (%EE = 62.6 ± 4.3) was attained with sulphate-containing LUV formulation (LUV_{DBCAS}), followed by pH gradient liposomes (LUV_{DBC5.5}, %EE = 31.0 ± 4.3) and conventional liposomes (LUV_{DBC7.4}, %EE = 27.9 ± 0.9). The %EE of LUV_{DBCAS} was significantly ($p < 0.001$) higher than any other tested formulation. According to Barenholz, ammonium sulphate dissociates inside of the vesicles, and NH₃ ions permeate out of the vesicles, leaving the protons (H⁺) inside, which keeps the acidification and thus the loading cycle.³⁴ Moreover, the sulphate counter-ion may complex with the weak base (DBC) to stabilise it inside the vesicles.³⁵ Such “extra” driving force (of the transmembrane ionic gradient) worked well for DBC upload in the sulphate-containing formulation. The low %EE of conventional liposomes was expected, since the DBC upload depends only on the drug locating in the lipid bilayer, while in the remote-loading technique the drug is actively loaded into the vesicles, in response to a pH/ion transmembrane gradient. However, the pH gradient formulation (LUV_{DBC5.5}) presented similar %EE of conventional liposomes, showing that the proton driving force (which is 80 times greater inside the liposomes (pH 5.5) than at the external medium (pH 7.4) was not enough to guarantee a satisfactory DBC encapsulation.

To demonstrate the advantage of the ionic-gradient liposomes, we calculated the trapped volume of the LUV_{DBCAS} formulation: 11 μL/μmol lipid (considering 380 nm vesicles and 5 mM total lipid). Such a value represents the total volume inside the gradient liposomes, and corresponds to ca. 6% of the total aqueous volume of the formulation.³⁶ Thus, the total DBC carried by the gradient liposomes corresponds to the liposomal bilayer-partitioned fraction, plus the charged DBC molecules trapped in the liposome volume.

In a liposome formulation, the amount of drug uploaded into the vesicles is directly correlated with the enhanced therapeutic efficacy achieved.³⁷ However, for local anaesthetics the maintenance of a fraction of non-entrapped drug is also advantageous, because the free LA will guarantee the fast onset of analgesia. For

example, in the LUV_{DBC}AS formulation, one third of the DBC remains free in solution to shorten the onset of action, while the encapsulated fraction (%EE = 62.6) can prolong the effect of anaesthesia.

In vitro dibucaine release from the liposomes

The *in vitro* DBC leakage from the liposomes was carried out under small dilution, simulating an infiltrative anaesthesia. Even though the *in vitro/in vivo* correlation is always difficult to prove, this experiment helped to assess the drug-release profile. The cumulative release of DBC (free and encapsulated in the liposome formulations) as a function of time is shown in Figure 3. The release of the control (free DBC) was completed in *ca.* 3 h, confirming the experiment was conducted under sink condition. The release profiles of DBC from the liposomes were treated with different mathematic models, being better described by the Weibull equation (eq. 2), as shown in Table 2. The curves were expressed by the negative b value, representing a parabolic curve with a steep initial slope followed by an exponential decay,³⁸ corresponding to the Fick diffusion and sustained release from the liposomes, respectively. The LUV_{DBC}AS formulation displayed the highest b-value (in module) among the liposome formulations, characterising the longest sustained release profile (50% \cong 7 h). These results agree well with the higher %EE of the sulphate-containing formulation, while conventional (LUV_{DBC}7.4) and pH gradient liposomes (LUV_{DBC}5.5), of equivalent encapsulation, showed similar release profiles (50% \cong 2 h). Probably, the DBC entrapped inside the LUV_{DBC}AS contributed greatly to sustainable release profile. A prolong LA release is desirable to improve potency of anaesthesia.⁷ Also; the full amount of drug is not released immediately upon injection which can reduce the risk of systemic toxicity.

Cell viability test

The cell viability of 3T3 cells treated with the DBC-loaded liposomes was tested *in vitro*, using the MTT assay. Figure 4 shows that the gradient liposomes (LUV AS and LUV 5.5) and LUV 7.4 without DBC, even at high nanoparticles concentration ($\sim 2.10^{12}$ liposomes/mL), do not significantly reduce cell viability when compared to the controls (non-treated cells).

The MTT cell viability assay was also performed for free DBC and the cytotoxic effect of the anaesthetic was found to be dose-dependent (Figure 4). The 300 μ M DBC dose led to a decrease in cell viability to $60.1 \pm 2.4\%$.

All the liposome dibucaine formulations (LUV_{DBC}7.4, LUV_{DBC}5.5, and LUV_{DBC}AS) were found to be significantly less cytotoxic than free DBC, at equivalent concentrations. The toxic effect of local anaesthetics is well known³⁹ and encapsulation in conventional⁴⁰ or ionic-gradient liposomes¹⁷ has been shown to reduce such intrinsic toxicity.

In vivo toxicity tests in zebrafish larvae

Since LUV_{DBC}AS was found the most promising formulation, based on the encapsulation efficiency and sustained release results, it was selected for further *in vivo* toxicity studies using the zebrafish model.

Zebrafish is a versatile vertebrate model organism that shows 70% genetic homology with humans, besides many physiological similarities to mammals.⁴¹ Additionally, many advantages make the zebrafish an interesting intermediate model between *in vitro* (cytotoxicity) and *in vivo* studies in mammals.⁴² This experimental design follows the so called “3Rs” (*reduce, refine and replace*) principle for investigations with animals.⁴³ Further, the zebrafish is increasingly used in nanoparticle toxicity studies because it allows the rapid evaluation of multiple biological parameters.^{44,45} According to He and colleagues,⁴⁶ numerous studies have confirmed that the toxicity profiles of zebrafish (*Danio rerio*) and mammals are extremely comparable. Therefore, *in vivo* toxicity tests were carried out with zebrafish larvae for LUV_{DBC}AS and free DBC.

Anaesthesia evaluation in zebrafish larvae

We initially tested to see if the zebrafish larvae were sensitive to the anaesthetic effect. The larvae were incubated for 2 h with an acute dose (32 μ M) of DBC. Two hours after treatment with DBC or LUV_{DBC}AS, all larvae were unable to move away from mechanical stimulus. This behaviour may be explained by the neuromuscular blocking effects the anaesthetic.⁴⁷ Most of the larvae treated with free DBC (93%) recovered from anaesthesia within 9 h (Figure 5A). However, only 58% of larvae treated with LUV_{DBC}AS reacted to stimulus, at 9 hpt. After 48 h (data not shown), some larvae (21%) from the ionic-gradient liposome formulation were still numb. These results provide evidence that zebrafish are sensitive upon exposure to DBC. Moreover, the prolonged anaesthetic effect achieved with the LUV_{DBC}AS formulation supported our hypothesis. Therefore, zebrafish larvae were considered to be a suitable model for further toxicity studies. No mortality was observed during the test.

Cardiotoxicity test

Local anaesthetics bind to voltage-gated sodium channels and prevent pain by blocking the initiation and propagation of the action potential in sensory nerves and other excitable cells.⁴⁸ Thus, the administration of LA may lead to systemic toxicity to cardiovascular and central nervous systems.⁴⁹

In the first days after fertilisation, zebrafish have already developed a heart with two cavities and a vascular system.⁵⁰ Here, we tested the cardiotoxicity effects of the long-term exposure to DBC on a 7 dpf larvae. As expected, free DBC decreases the heart rate compared to the control (untreated larvae), in doses higher than 2 μM (Figure 5B). The treatment with LUV_{DBC}AS did not significantly decrease the heart rate of the larvae, at any DBC dose tested. This result demonstrates that sulphate-gradient liposomes reduced DBC cardiotoxicity in zebrafish larvae. Such an effect can probably be explained by the slow release of DBC from the liposomes, attenuating its toxic effect. The use of zebrafish to assess the cardiotoxicity of active compounds is not a new concept. Milan and co-workers evaluated the effect of a hundred drugs on the heart rate of zebrafish. They found that all the compounds that induced QT interval prolongation in humans were also found to cause bradycardia and/or atrioventricular block in zebrafish larvae.⁵¹

Zebrafish motor behaviour

This test evaluated the behavioural effects of DBC on spontaneous swimming of zebrafish larvae at 4, 24 and 48 hpt. Figure 6A shows that at lower DBC doses (0.5 to 2 μM) free DBC and LUV_{DBC}AS did not significantly change larvae spontaneous movement (expressed as a percentage, relative to the control: untreated larvae). Larvae treated with 4 μM DBC presented hypoactivity at 4 hpt, but at 24 hpt and 48 hpt they showed hyperactive behaviour. This change of motor activity was not evident for LUV_{DBC}AS at 24 and 48 hpt. However, for larvae exposed to 8 μM DBC (free and encapsulated) only hypoactive behaviour was observed at 4 and 24 hpt⁵² studied the locomotor behaviour of larvae exposed to cocaine (5–50 μM). Surprisingly, only the hypoactive response was observed, in a dose-dependent manner. Those authors proposed that cocaine, as a local anaesthetic, first passes through the gills and skin and then blocks the peripheral nerves, suppressing locomotor activity. Here the treatment with 0.5–4 μM DBC did not cause deep anaesthesia, since the larvae were able to react to mechanical stimulus (data not shown). Therefore, any change in behaviour caused by DBC with the 0.5–4 μM doses can be related to DBC neurotoxicity, and LUV_{DBC}AS seemed to attenuate it. It is probable, that the hypoactive behaviour

presented by the larvae treated with 8 μM DBC (free or liposomal) was caused by neurotoxicity, but also by the peripheral anaesthetic effect.

Morphological changes

The observation of zebrafish malformations is widely used to perform developmental toxicity screening of compounds and nanoparticles.^{44,53} The larval transparency of zebrafish allows a direct evaluation of the toxicity.⁴⁶ In order to evaluate the LA toxicity, most of the cardiac and nervous system of the fish must be developed, which occurs in less than a week for zebrafish embryos.⁵⁴

The morphological changes after DBC treatment are represented in Figure 6B. DBC treatment caused evident abnormalities in the heart, brain, and jaw. In a similar way, other authors found abnormalities relating to the central nervous system, when larvae were treated with the antipsychotic²⁵ (risperidone) and antiepileptic⁵⁵ (valproic acid) drugs. An example of the abnormalities is shown in Figure S2 B (Supplementary Material). LUV_{DBC}AS significantly attenuated DBC-induced morphological changes, as shown in Figure S2 C. These data are in agreement with the cardiotoxicity results, showing that the sulphate liposome formulation reduces the DBC toxic effect.

Analgesia tests in mice (tail-flick)

Adequate postsurgical pain management is critical for patient rehabilitation¹. The infiltrative administration of local anaesthetics into the surgical site can achieve temporary analgesia, but bupivacaine and other long-acting agents provide no more than 7 hours of anaesthesia. To evaluate the extent of the analgesic effects of DBC, free and encapsulated into different liposome formulations, we performed the tail-flick test in male mice (Table 3). The sensory block duration induced by 320 μM of free DBC (11 h) was similar to the drug half-life time in rats.⁵⁶ LUV_{DBC}5.5 and LUV_{DBC}7.4 provided 13 h and 15 h of blockade, respectively. In addition, the AUEC values were significantly lower than that obtained with LUV_{DBC}AS. In fact, as long as 27 h of analgesia was registered with LUV_{DBC}AS, an outstanding result that corroborates the high %EE and prolonged *in vitro* release achieved with this formulation. LUV_{DBC}AS demonstrated that it can act as a repository, staying at the site of injection long enough to prolong the DBC effect. Therefore, a single dose of LUV_{DBC}AS formulation may provide long-term analgesia and a reduction in opioid demand in the postsurgical period.

Conclusions

Effective pain management after surgical procedures using long-acting local anaesthetics may reduce patient stress and opioid consumption. Dibucaine is a local anaesthetic which use is restricted to topical administration. Here we reported the successful development of novel liposome formulation (LUV_{DBC}AS) for the sustained release of dibucaine. The liposomes prepared with an ammonium sulphate gradient showed a higher encapsulation efficiency (2.3 times) than conventional liposomes. The prolonged analgesia time (27 h), displayed after infiltrative injection of the formulation (containing 320 µM DBC (or 0.012%) in mice, was in good agreement with the release profile determined at 37 °C (24 h). Both *in vitro* (3T3 cells in culture) and *in vivo* (zebrafish model) toxicity tests showed that encapsulation diminished the intrinsic toxicity of DBC. The zebrafish model was especially useful for evaluating both the local and systemic toxicities (as indicated by morphological changes, spontaneous movement and heartbeat rates) of the anaesthetic. It should be highlighted that the cardiotoxicity of DBC was markedly attenuated with the use of the LUV_{DBC}AS formulation. We propose the use of this ionic-gradient-based liposome formulation for the sustained release of dibucaine, providing long-term local anaesthesia with a single-dose infiltration, especially of interest during the postoperative surgical period.

Acknowledgements

This work was supported by Fapesp (#2013/13965-4, #2014/14457-5) and Capes (V.M.C. fellowship).

References

1. de Pinto M, Dagal A, O'Donnell B, Stogicza A, Chiu S, Edwards W. Regional anesthesia for management of acute pain in the intensive care unit. *Int J Crit Illn Inj Sci.* 2015;5(3):138-143. doi:10.4103/2229-5151.164917
2. Rawal N, Axelsson K, Hylander J, et al. Postoperative patient-controlled local anesthetic administration at home. *Anesth Analg.* 1998;86(1):86–89.
3. Ausems ME, Hulsewé KW, Hooymans PM, Hoofwijk AG. Postoperative analgesia requirements at home after inguinal hernia repair: effects of wound infiltration on postoperative pain*: Effects of wound infiltration on postoperative pain. *Anaesthesia.* 2007;62(4):325-331. doi:10.1111/j.1365-2044.2007.04991.x
4. Demiraran Y, Albayrak M, Yorulmaz IS, Ozdemir I. Tramadol and levobupivacaine wound infiltration at Cesarean delivery for postoperative analgesia. *J Anesth.* 2013;27(2):175-179. doi:10.1007/s00540-012-1510-7
5. Ozyilmaz K, Ayoglu H, Okyay RD, et al. Postoperative analgesic effects of wound infiltration with tramadol and levobupivacaine in lumbar disk surgeries. *J Neurosurg Anesthesiol.* 2012;24(4):331–335.

6. Grant MD, Gilbert J, Barenholz PD, Yechezkel, Bolotin PD, Elijah M, et al. A Novel Liposomal Bupivacaine Formulation to Produce Ultralong-Acting Analgesia. *Anesthesiology*. 2004;101(1):133-137.
7. de Paula E, Cereda CM, Fraceto LF, et al. Micro and nanosystems for delivering local anesthetics. *Expert Opin Drug Deliv*. 2012;9(12):1505-1524. doi:10.1517/17425247.2012.738664
8. de Paula E, Cereda C, Tofoli GR, Franz-Montan M, Fraceto LF, de Araújo DR. Drug delivery systems for local anesthetics. *Recent Pat Drug Deliv Formul*. 2010;4(1):23-34.
9. Gregoriadis G. Drug entrapment in liposomes. *FEBS Lett*. 1973;36(3):292-296.
10. Bangham AD, Standish MM, Watkins JC. Diffusion of univalent ions across the lamellae of swollen phospholipids. *J Mol Biol*. 1965;13(1):238-IN27. doi:http://dx.doi.org/10.1016/S0022-2836(65)80093-6
11. Pattni BS, Chupin VV, Torchilin VP. New Developments in Liposomal Drug Delivery. *Chem Rev*. 2015;115(19):10938-10966. doi:10.1021/acs.chemrev.5b00046
12. Kim J-S. Liposomal drug delivery system. *J Pharm Investig*. 2016;46(4):387-392. doi:10.1007/s40005-016-0260-1
13. Cern A, Golbraikh A, Sedykh A, Tropsha A, Barenholz Y, Goldblum A. Quantitative structure - property relationship modeling of remote liposome loading of drugs. *J Controlled Release*. 2012;160(2):147-157. doi:10.1016/j.jconrel.2011.11.029
14. Barenholz Y, Peer D. Liposomes and other assemblies as drugs and nano-drugs: From basic and translational research to the clinics. *J Controlled Release*. 2012;160(2):115-116. doi:10.1016/j.jconrel.2012.03.025
15. Fenske DB, Cullis, PR. *Encapsulation of drugs within liposomes by pH-gradient techniques*. Vol 2. London: In: Gregory Gregoriadis, Liposome Technology pp. 27-50; 2007.
16. Barenholz IY, Haran G. Method of amphiphatic drug loading in liposomes by pH gradient. 1993.
17. da Silva CMG, Fraceto LF, Franz-Montan M, et al. Development of egg PC/cholesterol/ α -tocopherol liposomes with ionic gradients to deliver ropivacaine. *J Liposome Res*. 2016;26(1):1-10. doi:10.3109/08982104.2015.1022555
18. da Silva CMG, Franz-Montan M, Limia CEG, et al. Encapsulation of ropivacaine in a combined (donor-acceptor, ionic-gradient) liposomal system promotes extended anesthesia time. *PLOS ONE*. 2017;12(10):e0185828. doi:10.1371/journal.pone.0185828
19. Cousins MJ, Bridenbaugh PO, Carr DB, Horlocker TT. *Cousins and Bridenbaugh's Neural Blockade in Clinical Anesthesia and Pain Medicine*. 4th ed. Philadelphia: Wolters Kluwer Health; 2012. <https://books.google.com.br/books?id=UoHb8iUgvsC>.
20. Covino BG, Vassallo HG. *Local Anesthetics: Mechanics of Action and Clinical Use*. New York: Grune & Stratton; 1976.
21. Beiranvand S, Eatemadi A, Karimi A. New Updates Pertaining to Drug Delivery of Local Anesthetics in Particular Bupivacaine Using Lipid Nanoparticles. *Nanoscale Res Lett*. 2016;11(1). doi:10.1186/s11671-016-1520-8
22. Malik O, Kaye AD, Kaye A, Belani K, Urman RD. Emerging roles of liposomal bupivacaine in anesthesia practice. *J Anaesthesiol Clin Pharmacol*. 2017;33(2):151-156. doi:10.4103/joacp.JOACP_375_15

23. Barbosa RM, Silva CMG da, Bella TS, et al. Cytotoxicity of solid lipid nanoparticles and nanostructured lipid carriers containing the local anesthetic dibucaine designed for topical application. *J Phys Conf Ser.* 2013;429:012035. doi:10.1088/1742-6596/429/1/012035
24. Mendyk A, Jachowicz R. Unified methodology of neural analysis in decision support systems built for pharmaceutical technology. *Expert Syst Appl.* 2007;32(4):1124-1131. doi:10.1016/j.eswa.2006.02.019
25. Igartúa DE, Calienni MN, Feas DA, Chiaramoni NS, Alonso SDV, Prieto MJ. Development of Nutraceutical Emulsions as Risperidone Delivery Systems: Characterization and Toxicological Studies. *J Pharm Sci.* 2015;104:4142–4152.
26. Panzica-Kelly JM, Zhang CX, Danberry TL, et al. Morphological score assignment guidelines for the dechorionated zebrafish teratogenicity assay. *Birth Defects Res B Dev Reprod Toxicol.* 2010;89(5):382-395. doi:10.1002/bdrb.20260
27. D'Amour FE, Smith DL. A method for determining loss of pain sensation. *J Pharmacol Exp Ther.* 1941;72(1):74.
28. Brazeau G, Sauberan SL, Gatlin L, Wisniecki P, Shah J. Effect of particle size of parenteral suspensions on *in vitro* muscle damage. *Pharm Dev Technol.* 2011;16(6):591-598. doi:10.3109/10837450.2010.542161
29. Filipe V, Hawe A, Jiskoot W. Critical Evaluation of Nanoparticle Tracking Analysis (NTA) by NanoSight for the Measurement of Nanoparticles and Protein Aggregates. *Pharm Res.* 2010;27(5):796-810. doi:10.1007/s11095-010-0073-2
30. Wong J, Brugger A, Khare A, et al. Suspensions for intravenous (IV) injection: A review of development, preclinical and clinical aspects. *Adv Drug Deliv Rev.* 2008;60(8):939-954. doi:10.1016/j.addr.2007.11.008
31. Kuroda Y, Ogawa M, Nasu H, et al. Locations of local anesthetic dibucaine in model membranes and the interaction between dibucaine and a Na⁺ channel inactivation gate peptide as studied by 2H- and 1H-NMR spectroscopies. *Biophys J.* 1996;71(3):1191-1207.
32. Ribeiro LNM, Franz-Montan M, Breikreitz MC, et al. Nanostructured lipid carriers as robust systems for topical lidocaine-prilocaine release in dentistry. *Eur J Pharm Sci.* 2016;93:192-202. doi:10.1016/j.ejps.2016.08.030
33. Kučerka N, Nieh M-P, Katsaras J. Fluid phase lipid areas and bilayer thicknesses of commonly used phosphatidylcholines as a function of temperature. *Biochim Biophys Acta BBA - Biomembr.* 2011;1808(11):2761-2771. doi:https://doi.org/10.1016/j.bbamem.2011.07.022
34. Barenholz Y. *Amphipathic Weak Base Loading into Preformed Liposomes Having a Transmembrane Ammonium Ion Gradient.* Vol 2. London: In: Gregory Gregoriadis, Liposome Technology pp. 01-22; 2007.
35. Gubernator J. Active methods of drug loading into liposomes: recent strategies for stable drug entrapment and increased *in vivo* activity. *Expert Opin Drug Deliv.* 2011;8(5):565-580. doi:10.1517/17425247.2011.566552
36. Mantripragada S. A lipid based depot (DepoFoam® technology) for sustained release drug delivery. *Prog Lipid Res.* 2002;41(5):392-406. doi:10.1016/S0163-7827(02)00004-8
37. Cohen R, Steiner A, Kanaan H, Barenholz Y. Chemical and physical characterization of remotely loaded bupivacaine liposomes: comparison between large multivesicular vesicles and small unilamellar vesicles. *J Mater Chem B.* 2013;1(36):4619-4627. doi:10.1039/c3tb20609b

38. Arifin DY, Lee LY, Wang C-H. Mathematical modeling and simulation of drug release from microspheres: Implications to drug delivery systems. *Adv Drug Deliv Rev.* 2006;58(12-13):1274-1325. doi:10.1016/j.addr.2006.09.007
39. Tarba C, Crăciun C. A comparative study of the effects of procaine, lidocaine, tetracaine and dibucaine on the functions and ultrastructure of isolated rat liver mitochondria. *Biochim Biophys Acta BBA - Bioenerg.* 1990;1019(1):19-28. doi:10.1016/0005-2728(90)90120-S
40. de Araújo DR, Cereda CMS, Brunetto GB, et al. Pharmacological and local toxicity studies of a liposomal formulation for the novel local anaesthetic ropivacaine. *J Pharm Pharmacol.* 2008;60(11):1449-1457. doi:10.1211/jpp/60.11.0005
41. Barbazuk WB, Korf I, Kadavi C, et al. The Syntenic Relationship of the Zebrafish and Human Genomes. *Genome Res.* 2000;10(9):1351-1358.
42. Lee KY, Jang GH, Byun CH, Jeun M, Searson PC, Lee KH. Zebrafish models for functional and toxicological screening of nanoscale drug delivery systems: promoting preclinical applications. *Biosci Rep.* 2017;37(3):BSR20170199. doi:10.1042/BSR20170199
43. Russell WMS, Burch RL, Hume CW. The principles of humane experimental technique. 1959.
44. Chakraborty C, Sharma AR, Sharma G, Lee S-S. Zebrafish: A complete animal model to enumerate the nanoparticle toxicity. *J Nanobiotechnology.* 2016;14:65(1). doi:10.1186/s12951-016-0217-6
45. Truong L, Simonich MT, Saili KS, Tanguay RL. Fishing to Design Inherently Safer Nanoparticles. In: *Zebrafish.* John Wiley; 2011:283–293. <http://dx.doi.org/10.1002/9781118102138.ch20>.
46. He J-H, Guo S-Y, Zhu F, et al. A zebrafish phenotypic assay for assessing drug-induced hepatotoxicity. *J Pharmacol Toxicol Methods.* 2013;67(1):25-32. doi:10.1016/j.vascn.2012.10.003
47. Valentim AM, Félix LM, Carvalho L, Diniz E, Antunes LM. A New Anaesthetic Protocol for Adult Zebrafish (*Danio rerio*): Propofol Combined with Lidocaine. *PLOS ONE.* 2016;11(1):1-12. doi:10.1371/journal.pone.0147747
48. Catterall WA, Swanson TM. Structural Basis for Pharmacology of Voltage-Gated Sodium and Calcium Channels. *Mol Pharmacol.* 2015;88(1):141-150. doi:10.1124/mol.114.097659
49. Mather LE, Copeland SE, Ladd LA. Acute toxicity of local anesthetics: underlying pharmacokinetic and pharmacodynamic concepts. *Reg Anesth Pain Med.* 2005;30(6):553–566.
50. Rubinstein AL. Zebrafish assays for drug toxicity screening. *Expert Opin Drug Metab Toxicol.* 2006;2(2):231-240. doi:10.1517/17425255.2.2.231
51. Milan DJ, Paterson TA, Ruskin JN, Peterson RT, MacRae CA. Drugs That Induce Repolarization Abnormalities Cause Bradycardia in Zebrafish. *Circulation.* 2003;107(10):1355-1358. doi:10.1161/01.CIR.0000061912.88753.87
52. Kirla KT, Groh KJ, Steuer AE, et al. From the Cover: Zebrafish Larvae Are Insensitive to Stimulation by Cocaine: Importance of Exposure Route and Toxicokinetics. *Toxicol Sci.* 2016;154(1):183-193. doi:10.1093/toxsci/kfw156
53. Haldi M, Harden M, D'Amico L, DeLise A, Seng WL. Developmental Toxicity Assessment in Zebrafish. In: *Zebrafish.* John Wiley; 2011:15–25. doi:10.1002/9781118102138.ch2
54. Kimmel CB, Ballard WW, Kimmel SR, Ullmann B, Schilling TF. Stages of embryonic development of the zebrafish. *Dev Dyn.* 1995;203(3):253–310.

55. Feas DA, Igartúa DE, Calienni MN, et al. Nutraceutical emulsion containing valproic acid (NE-VPA): a drug delivery system for reversion of seizures in zebrafish larvae epilepsy model. *J Pharm Investig.* 2017;47:429-437. doi:10.1007/s40005-017-0316-x
56. Igarashi K, Kasuya F, Fukui M. Metabolism of dibucaine. II. Disposition and metabolism of dibucaine in rats. *J Pharmacobiodyn.* 1989;12:523-529.

ACCEPTED MANUSCRIPT

FIGURE CAPTIONS

Figure 1: Timeline of *in vivo* toxicity experiments during zebrafish development. Numbers represent the day post fertilization (dpf) of larvae. Larvae were treated at 5 dpf with free DBC or with the liposome formulation (with or without DBC). The motor behavior test was performed after 4h, 24h and 48 h post treatment (hpt). Heart rate changes and morphological tests were performed at 7 dpf, after 48 hpt.

Figure 2: Characterization of different liposomal DBC formulations during six months of storage at 4 °C, as measured by DLS. Average size (bars) and PDI (gray lines) of: (A) LUV 7.4 and LUV_{DBC}7.4; (B) LUV 5.5 and LUV_{DBC}5.5; (C) LUV AS and LUV_{DBC}AS. In (D): Zeta potential values measured for all formulations. Statistical Student's t Test (paired) was applied to compare liposome formulations at initial (0 day) vs. time (*p<0.05).

Figure 3: Cumulative drug release of DBC from liposomal formulations and free DBC (in solution), at pH 7.4 and 37 °C. Results were expressed as the mean ± SD (n=6).

Figure 4: Cell viability of BALB/c 3T3 fibroblasts treated with liposomes and DBC (free or encapsulated in liposomes), for 2 hours, as measured by the MTT assay. Results are expressed as the mean ± SEM (n=3). Statistical analysis was performed by One-way ANOVA and Tukey post-hoc test. Statistical significance: *p<0.03, **p<0.01, ***p< 0.0005 and ****p<0.0001, for liposomal formulations vs. free DBC at the same concentration.

Figure 5: A) Percentage of larvae recovery from anesthesia after 2-hour treatment with 32 µM DBC (free and encapsulated in LUV_{DBC}AS. hpt = hours post treatment. (n= 24). B) Heart beats rates of zebrafish larvae treated with liposome (with or without DBC) formulations or free DBC (n=8). Data was recorded 48 hours post treatment. Non-treated larvae were used as control. Results are expressed as the mean ± SEM. Statistical analysis was performed by 1-way-ANOVA/Dunnett with significance of *p<0.05; **p<0.01, ***p< 0.001 and ****p<0.0001, compared to the control.

Figure 6: A) Percentage of spontaneous movement of zebrafish larvae treated with dibucaine (free or encapsulated in LUV_{DBC}AS) for 4, 24 and 48 (n = 24). Statistical analysis was performed by One-way ANOVA/Dunnett with significance of *p<0.05; **p<0.01, ***p< 0.001 and ****p<0.0001, compared to the control (non-treated larvae). B) Percentage of morphological changes after treatment with 8 µM of DBC (free or encapsulated in LUV_{DBC}AS), in respect to the control for: tail, heart, face, brain, and jaw of the zebrafish larvae. Results were expressed as the mean ± SEM. Statistical analysis was performed by One-way ANOVA/Dunnett with significance of *p<0.05; **p<0.01, ***p< 0.001 and ****p<0.0001, compared to the control (non-treated larvae).

Figure captions - Supplementary material

Figure S1: Characterization of liposome DBC formulations over time (180 days of storage at 4 °C), as measured by nanotracking analysis. Nanoparticles size (bars) and concentration (gray lines) for: A) LUV 7.4 and LUV_{DBC}7.4; B) LUV 5.5 and LUV_{DBC}5.5; C) LUV AS and LUV_{DBC}AS.

Figure S2: Lateral view of 7dpf larvae treated for 48 hours with **A**: control; **B**: DBC 8 µM; **C**: LUV_{DBC}AS 8 µM; **D**: LUV AS. Details observed in **A**: Lateral view of normal LJ (lower jaw); FB (forebrain); MB (midbrain); HB (hindbrain); H (heart); OC (otic capsule). **B**: Representative score assignment of heart (Score 2) - atrium and ventricle chambers are severely enlarged (circle), misshaped, and not well defined. Face (Score 2) - increased space between the midbrain and otic capsule (dotted), small and not well-defined olfactory region. Brain (Score 2) - irregular forebrain and midbrain shapes without well-defined brain portion junctions (arrows). Jaw (Score 2) irregular shaped lower (line) and upper jaw. **C**: Heart (Score 4) - normal heart morphology with a slightly smaller ventricle (arrow). Brain (Score 4) - slightly smaller forebrain region (line). **D**: tail is slightly curved (arrow). The assay is based on morphological anomalies using the numerical score system proposed by Panzica-Kelly and coworkers.²⁶

Table 1. Dibucaine encapsulation efficiency (%EE) and size distribution (mean \pm SD) of liposome formulations (with and without dibucaine), as measured by dynamic light scattering (DLS) and nanoparticle tracking analysis (NTA) in freshly prepared samples.

Formulation	DLS	NTA (nm)			Number of particles ($\times 10^{12}$ /mL)	EE (%)
	(nm)	D90	D50	D10		
LUV 7.4	345 \pm 5	308 \pm 17	179 \pm 7	107 \pm 3	1.9 \pm 0.2	-
LUV _{DBC} 7.4	352 \pm 3	292 \pm 24	164 \pm 8	98 \pm 6	2.2 \pm 0.1	27.9 \pm 0.9
LUV 5.5	386 \pm 6	210 \pm 7	141 \pm 6	82 \pm 1	1.5 \pm 0.2	-
LUV _{DBC} 5.5	438 \pm 5*	305 \pm 13*	165 \pm 10*	100 \pm 4*	2.2 \pm 0.1	31.0 \pm 4.3
LUV AS	374 \pm 11	273 \pm 5	162 \pm 6	99 \pm 3	3.3 \pm 0.1	-
LUV _{DBC} AS	412 \pm 18*	331 \pm 6*	186 \pm 6*	104 \pm 4	3.9 \pm 0.2	62.6 \pm 4.3

Statistics ($n = 3$) - unpaired Student's test; comparison between each liposome formulation, with vs. without DBC (* $p < 0.05$).

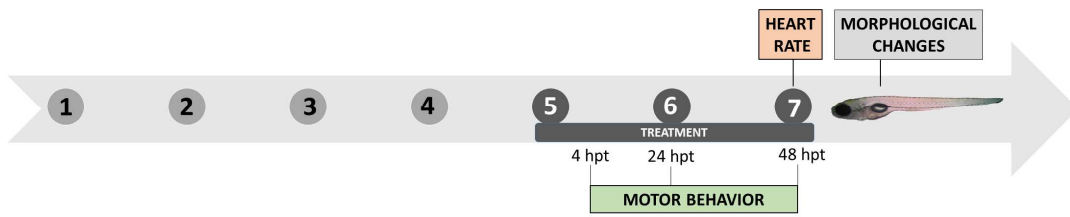
Table 2. Kinetic parameters measured for the release of dibucaine from liposome formulations, according to the Weibull treatment (see equation 2).

Formulation	r^2	a	b
LUV _{DBC} 7.4	0.914	1.32	- 6.31
LUV _{DBC} 5.5	0.944	1.11	- 5.59
LUV _{DBC} AS	0.990	1.04	- 6.48

Table 3. Area under the curve (AUC) of sensorial blockade on the mice tail induced by DBC (320 μ M) in solution or encapsulated into liposomes (n=7).

Formulation	AUC (mean \pm SD)	Duration of analgesia (h)
free DBC	769.4 \pm 61.6	11
LUV _{DBC} 7.4	947.7 \pm 113.0	15
LUV _{DBC} 5.5	831.4 \pm 78.2	13
LUV _{DBC} AS	1665.9 \pm 112.5 ^{a,b,c***}	27

Statistics: ANOVA/Tukey ($p < 0.001$)***. a. free DBC vs LUV_{DBC}AS; b. LUV_{DBC}7.4 vs LUV_{DBC}AS; c. LUV_{DBC}5.5 vs LUV_{DBC}AS.



ACCEPTED MANUSCRIPT

